The acoustic velocity, refractive index, and equation of state of liquid ammonia dihydrate under high pressure and high temperature

Cite as: J. Chem. Phys. **137**, 104504 (2012); https://doi.org/10.1063/1.4751944
Submitted: 22 May 2012 . Accepted: 27 August 2012 . Published Online: 12 September 2012

Chunli Ma, Xiaoxin Wu, Fengxian Huang, Qiang Zhou, Fangfei Li, and Qiliang Cui

The acoustic velocity, refractive index, and equation of state of liquid ammonia dihydrate under high pressure and high temperature

Chunli Ma, Xiaoxin Wu, Fengxian Huang, Qiang Zhou, Fangfei Li,[a] and Qiliang Cui
State Key Laboratory of Superhard Materials, Jilin University, Changchun, 130012 People's Republic of China

(Received 22 May 2012; accepted 27 August 2012; published online 12 September 2012)

High-pressure and high-temperature Brillouin scattering studies have been performed on liquid of composition corresponding to the ammonia dihydrate stoichiometry ($NH_3 \cdot 2H_2O$) in a diamond anvil cell. Using the measured Brillouin frequency shifts from 180° back- and 60° platelet-scattering geometries, the acoustic velocity, refractive index, density, and adiabatic bulk modulus have been determined under pressure up to freezing point along the 296, 338, 376, and 407 K isotherms. Along these four isotherms, the acoustic velocities increase smoothly with increasing pressure but decrease with the increased temperature. However, the pressure dependence of the refractive indexes on the four isotherms exhibits a change in slope around 1.5 GPa. The bulk modulus increases linearly with pressure and its slope, dB/dP, decreases from 6.83 at 296 K to 4.41 at 407 K. These new datasets improve our understanding of the pressure- and temperature-induced molecular structure changes in the ammonia-water binary system. © *2012 American Institute of Physics*. [http://dx.doi.org/10.1063/1.4751944]

I. INTRODUCTION

The ammonia-water binary system is of great theoretical, physical, and biological importance.[1,2] And as a component of the outer solar system gas-giant planets (Uranus and Neptune) and their large satellites (e.g., Triton and Titan), the ammonia-water binary system has drawn much attention from planetary scientists. The properties of the outer planets and large satellites are related to the behavior of ammonia hydrates over the pressure and temperature ranges in their interior. Therefore, molecular dynamics simulations and neutron diffraction studies have provided insights into the ammonia-water system at similar conditions to these planetary environments.[3–10] These studies are dedicated in determining new crystal structures and their relationship in P, T space (phase diagrams). The equation of state (EOS) of two solid phases, ammonia monohydrate phase I (AMH I) and ammonia dihydrate phase I (ADH I), have been determined.

It has also been known that the stoichiometric ammonia hydrates are the simplest to contain hetero- and homonuclear hydrogen bonds,[11] and the bonding will display a series of dramatic changes upon application of pressure. The latest studies have reported surprising results, showing that a liquid with the ammonia *mono*hydrate stoichiometry compressed at 3.5 GPa at room temperature freezes to form a mixture of high-pressure ammonia *hemi*hydrates (phase II), which has monoclinic symmetry, and ice VII.[12] The phase mixture of ammonia *mono*hydrate and ice are also obtained by warming ammonia *di*hydrate at high pressure.[6,13] We have found that liquid with the ammonia *hemi*hydrate stoichiometry freezes to a crystal with orthorhombic symmetry at 3.5 GPa at room temperature, and experiences two further solid-solid phase transitions under higher pressure conditions.[14] Given this remarkable complexity as a function of pressure, temperature, and composition, it is necessary to make a comprehensive study of the ammonia-water binary system, from which we may supplement the understanding of hydrogen bonding changes in ammonia hydrates, and thus help to explore the physical state of the outer planets and large satellites.

Brillouin scattering is a useful optical way to investigate the acoustic velocity, refractive index, and elastic properties of various materials in diamond anvil cell, allowing the EOS of materials to be determined. In this work, the Brillouin frequency shifts of liquid with the ammonia *di*hydrate stoichimetry ($NH_3 \cdot 2H_2O$) have been obtained from 180° back- and 60° platelet-scattering geometries along four isotherms, 296, 338, 376, and 407 K under high pressure. Hence, the acoustic velocity and refractive indexes of liquid ammonia *di*hydrate under high-pressure and high-temperature conditions are obtained, and the EOS of liquid ammonia *di*hydrate is further determined in our experimental pressure and temperature scope, which have greatly extended the pressure and temperature range of observations reported by Croft *et al.* on this potentially important planetary fluid.[15] The adiabatic bulk modulus along these four isotherms are also presented and compared with respect to our previous results for pure ammonia and pure water. The reason for the highest acoustic velocity of liquid ammonia *di*hydrate at 407 K is further discussed. These new datasets will be helpful to widely understand possible pressure- and temperature-induced molecular structure changes in the ammonia-water binary system.

II. EXPERIMENTAL METHODS

The liquid mixture of ammonia and water (molar ratio is 1:2) was prepared by two procedures: (1) condensing ammonia gas into an evacuated aluminum container, which was

[a]Author to whom correspondence should be addressed. Electronic mail: lifangfei@jlu.edu.cn.

cooled to 220 K in low temperature alcohol bath; (2) the condensed ammonia was weighted and diluted with de-ionized water to appropriate stoichiometry (33.33 mol. % NH_3). Finally, this mixture of liquid ammonia and de-ionized water was sealed in a polytetrafluoroethylene (PTFE)-lined stainless steel reactor at 220 K. Upon gradual warming to room temperature, the solution was shaken to reach a homogeneous state, and then stored in a refrigerator for later study. The high-pressure Brillouin scattering measurement was performed with a modified Merrill–Bassett type four-screw diamond anvil cell (DAC) with large conical opening aperture.[16] The culet size of diamond anvils was 400 μm, a tungsten gasket was pre-indented, and a 120 μm hole was drilled in the indent center to form a sample chamber. The sample, together with one ruby ball with diameter about 10 μm, was loaded into the gasketed DAC at low temperature. After sample was loaded into DAC chamber, Raman spectrum was measured in several different places, which present identical feature in all spectra, to confirm the homogeneous state in liquid.

The pressure was calibrated by the ruby R_1 fluorescence line.[17] The precision of pressure measured in the high-pressure and high-temperature experiments was estimated to 0.05 GPa. The DAC was externally heated using a resistance heater and temperature was measured by a Chromel-Almel thermocouple attached to the side face of the diamond. The temperature was controlled by feed-back power and the variation was less than 1 K during the collecting of Brillouin spectra. Taking into account the existence of temperature gradient around the sample chamber, the temperature dispersion between the anvil center and the side face of the diamond should be considered and corrected properly. Within the temperature and pressure range of this study, it was assumed that the temperature dependence of ruby fluorescence shifts was independent of pressure.[18] Before the sample was loaded into sample chamber, only one ruby ball was placed in the sample chamber center. Then increasing heating power at ambient pressure to record the ruby R_1 fluorescence can be converted to temperature according to Ref. 18, reflecting the exact condition at sample chamber position; therefore, the thermocouple read temperature is correlated with the ruby fluorescence converted temperature. This relation was used to revise the temperature in sample chamber center before each constant temperature experiments. This correction method ensures that we get accurate temperature and pressure measurements as have been done in Refs. 19 and 20.The sample was then heated to a constant temperature and the pressure was calibrated and gradually increased till crystallization. The solidification process was monitored visually through a microscope; the solidification pressures of the four isotherms agree with the high-pressure phase diagrams of Boone.[21]

The 532 nm laser was used as Brillouin excitation source, which was generated by a single-mode diode-pumped Nd: Vanadate laser (Coherent Company). The Brillouin spectra were collected by a 3+3 pass tandem Fabry–Perot interferometer.[22] To obtain acoustic velocity and refractive index, both 180° back-scattering and 60° platelet-scattering geometry measurements were performed. In 180° back-scattering geometry, the modulus of the phonon wavevector is equal to $|q| = 2nk$, with q is wavevector of the phonon and k is the wavevector of the photon, the Brillouin frequency shifts $\Delta\omega$ are related to the acoustic velocities V as follows:[23]

$$\Delta\omega_{180} = \frac{2nV_{180}}{\lambda_0}, \tag{1}$$

where λ_0 is the wavelength of the exciting radiation and n is the sample refractive index. In 60° platelet-scattering geometry, the modulus of the phonon wavevector is equal to $|q| = 2nk\mathrm{Sin}\theta_0 = 2k\mathrm{Sin}\theta$. As description is shown in Ref. 19, $2\theta_0$ is the angle between incident light and scattered light in the sample, while 2θ is the angle between incident light and scattered light out of DAC. Here, if $2\theta = 60°$, then the Brillouin frequency shifts $\Delta\omega$ for 60° platelet-scattering is expressed as

$$\Delta\omega_{60} = \frac{V_{60}}{\lambda_0}. \tag{2}$$

Obviously, in platelet geometry acoustic velocities can be calculated without the knowledge of sample refractive index, and since the velocity is independent of the direction in liquid, $V_{180} = V_{60}$, the refractive index of liquid sample can be obtained at each pressure, with n in proportion to the ratio of Brillouin frequency shift.[19,23,24]

III. RESULTS AND DISCUSSION

A. Brillouin scattering spectra and error analysis

Pressure dependence of the Brillouin frequency shifts from liquid $NH_3 \cdot 2H_2O$ was collected along 296, 338, 376, and 407 K isotherms in back and platelet geometries. Figure 1 shows representative Brillouin spectra in platelet geometry at different pressures and room temperature

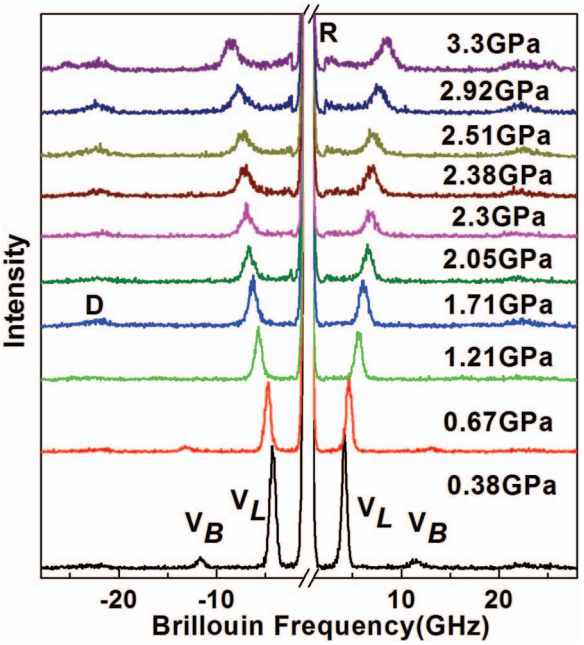

FIG. 1. Brillouin spectra of liquid $NH_3 \cdot 2H_2O$ at 296 K measured in platelet-scattering geometry. *R* is the peak of Rayleigh scattering; D refers to diamond peak; V_L indicates the longitudinal signal from liquid ammonia *di*hydrate; V_B indicates the weak backscattering signal. The liquid $NH_3 \cdot 2H_2O$ begins to solidify at 2.92 GPa, as monitored by microscope observations.

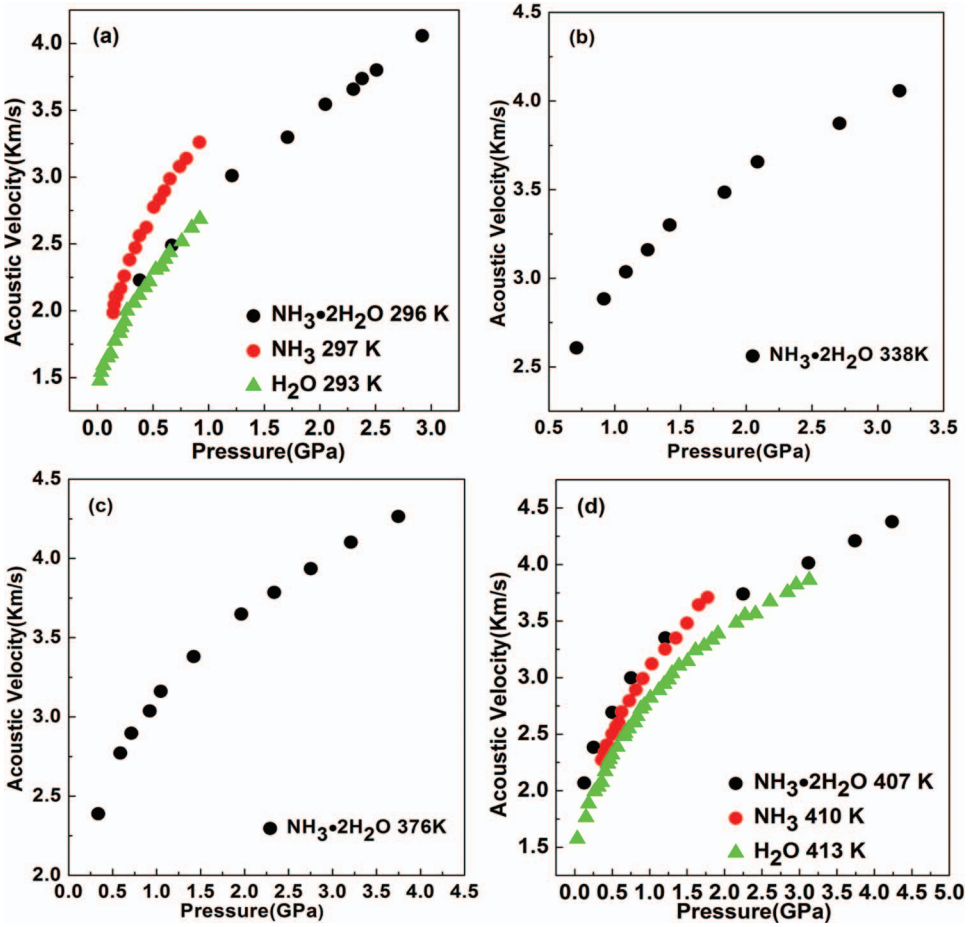

FIG. 2. The acoustic velocity of liquid $NH_3 \cdot 2H_2O$ as a function of pressure at different temperatures: (a) 296 K; (b) 338 K; (c) 376 K; and (d) 407 K. The pressure dependence of acoustic velocities in pure ammonia and pure water is shown at similar temperature in (a) and (d), respectively. Red solid circles represent ammonia and green triangles represent water. In (a), the temperature of the ammonia is 297 K and of the water is 293 K; in (d), the temperature of the ammonia is 410 K and of the water is 413 K.

(296 K). The Brillouin spectra are of good quality with a high signal-to-noise ratio. In a homogeneous liquid, no shear wave velocity can be detected; there should be only one longitudinal signal (V_L shown in Figure 1) detected in $NH_3 \cdot 2H_2O$, which shifts monotonously with increasing pressure up to the solidification point. However, because parts of incident laser are reflected from the downstream diamond anvil and serves as the backscattering incident light, a pair of weak backscattering signal (V_B) is observed in the 60° platelet-scattering spectra simultaneously. Notably, this weak but clear backscattering frequency shift (V_B) appearing in the 60° platelet-scattering spectra gives the value identical to that shown in a 180° back-scattering spectra.

The angle configuration of external Brillouin optical system is determined by planar mirror through optical principal of reflection. The angle uncertainty is 0.2° for the external light path, so such small uncertainty will lead to negligible systematic errors in our work. Using diamond anvil cell in the high-pressure Brillouin scattering experiment, the non-parallel diamond anvil surfaces will result in systematic measurement errors. These kind of errors have been discussed by Zouboulis,[25] which can also be neglected in this work. The uncertainty in the direction of phonon propagation relative to crystalline axes of any solid crystal specimen in the ray path will cause errors, however, this type of error is not applicable to isotropic liquid $NH_3 \cdot 2H_2O$. In this work, the major sources of errors are random errors, which come from statistical noise in the collected spectra and the resulting imprecision in the magnitude of Brillouin frequency shifts. These are greatly reduced by a longer time accumulation for each spectrum and by application of Lorentz analysis to the curve fitting procedure. The final relative uncertainty of Brillouin frequency shift in this investigation is better than 2%.

B. Acoustic velocity and refractive index

According to Eq. (2), the acoustic velocities of $NH_3 \cdot 2H_2O$ have no relation with the refractive index n in platelet geometry measurements and can be calculated directly.[24] The liquid $NH_3 \cdot 2H_2O$ acoustic velocity (V_L) as a function of pressure at four constant temperatures is shown in Figure 2, as also listed in Table I. Pressure has a larger effect than temperature on the variation of acoustic velocity. The acoustic velocities of $NH_3 \cdot 2H_2O$ increase smoothly with increasing pressure at a constant temperature. For comparison, the pure ammonia and pure water acoustic velocities

TABLE I. Brillouin frequency shift ($\Delta\omega$), sound velocity (V), refraction index (n), density (ρ), and bulk modulus (B) of liquid ammonia *di*hydrate ($NH_3 \cdot 2H_2O$) at various pressures and temperatures; the freezing pressure at different temperatures are denoted by star on top right corner.

P (GPa)	$\Delta\omega_{60^\circ}$ (GHz)	$\Delta\omega_{180^\circ}$ (GHz)	V (Km/s)	n	ρ (g/cm^3)	B (GPa)
			296 K			
0.38	4.188	11.587	2.229	1.383	0.941	4.674
0.67	4.677	13.113	2.489	1.402	0.981	6.079
1.21	5.658	16.299	3.011	1.440	1.063	9.637
1.71	6.198	18.232	3.298	1.471	1.126	12.253
2.05	6.661	19.995	3.544	1.501	1.188	14.921
2.3	6.873	21.002	3.658	1.528	1.241	16.600
2.38	7.023	21.513	3.737	1.532	1.249	17.438
2.51	7.142	22.064	3.800	1.545	1.274	18.400
2.92*	7.625	24.265	4.057	1.591	1.363	22.433
			338 K			
0.71	4.899	13.770	2.607	1.405	0.989	6.720
0.92	5.419	15.324	2.884	1.414	1.007	8.375
1.09	5.706	16.323	3.037	1.430	1.042	9.607
1.25	5.940	17.091	3.161	1.439	1.060	10.586
1.42	6.202	18.019	3.300	1.453	1.089	11.861
1.84	6.550	19.209	3.486	1.466	1.117	13.572
2.09	6.872	20.493	3.657	1.491	1.168	15.614
2.71	7.279	22.235	3.874	1.527	1.240	18.605
3.17*	7.625	24.194	4.058	1.587	1.354	22.290
			376 K			
0.59	5.208	14.655	2.771	1.407	0.992	7.621
0.71	5.443	15.356	2.897	1.411	1.000	8.390
0.92	5.708	16.235	3.038	1.422	1.025	9.454
1.05	5.940	16.966	3.161	1.428	1.037	10.364
1.42	6.354	18.321	3.381	1.442	1.066	12.186
1.96	6.857	20.166	3.649	1.471	1.126	14.988
2.34	7.114	21.221	3.786	1.492	1.169	16.748
2.75	7.396	22.296	3.936	1.507	1.200	18.593
3.21	7.710	23.647	4.103	1.533	1.252	21.077
3.75*	8.014	24.979	4.265	1.558	1.300	23.653
			407 K			
0.25	4.481	12.349	2.385	1.378	0.929	5.284
0.50	5.059	14.053	2.692	1.389	0.953	6.909
0.75	5.635	15.850	2.998	1.407	0.991	8.912
1.21	6.298	17.981	3.351	1.428	1.036	11.639
2.24	7.027	20.601	3.739	1.466	1.117	15.607
3.12	7.544	22.663	4.014	1.502	1.190	19.175
3.74	7.909	24.051	4.209	1.520	1.226	21.724
4.24*	8.230	25.262	4.380	1.535	1.255	24.064

as a function of pressure are presented in Figure 2(a).[16,19] At room temperature, the acoustic velocity of $NH_3 \cdot 2H_2O$ locates between the values for pure ammonia and pure water, being slightly higher than those of water. Figure 2(d) shows the pressure dependence of both pure ammonia and pure water acoustic velocities at 410 and 413 K, respectively. When the temperature is increased up to 407 K, the difference between the $NH_3 \cdot 2H_2O$ and pure water acoustic velocity becomes larger, the acoustic velocity of $NH_3 \cdot 2H_2O$ becomes even greater than pure ammonia. The variation of the $NH_3 \cdot 2H_2O$ acoustic velocities at constant temperature with increasing pressure is similar to that of water.

The back- and platelet-scattering geometries provided us with an opportunity to obtain the refractive index, using the ratio of the Brillouin scattering frequency shifts (Eqs. (1) and (2)); this being proportional to $\Delta\omega_{180^\circ}/\Delta\omega_{60^\circ}$. The refractive index of liquid $NH_3 \cdot 2H_2O$ is then plotted as a function of pressure at 296, 338, 376, and 407 K in Figure 3. The refractive indexes as a function of pressure on each isotherm exhibit a change in slope around 1.5 GPa. Though the refractive index along each isotherm increases smoothly with increasing pressure, the slopes of the refractive index, dn/dP, look very similar along each of the four isotherms below 1.5 GPa, that is, they are approximately parallel as a function of pressure. However, above 1.5 GPa, the slopes diverge: at 296 K, the slope increases (dn/dP become larger with pressure), while at 407 K, the slope becomes substantially shallower. This behavior differs from pure ammonia and water, where the refractive index increases smoothly with increasing pressure along isotherms and decreases with the increasing temperature.[16,19] This behavior in $NH_3 \cdot 2H_2O$ may be indicative of a change in the structure of the liquid, perhaps associated with the pressure-induced dehydration seen in the solid phases at these pressures.

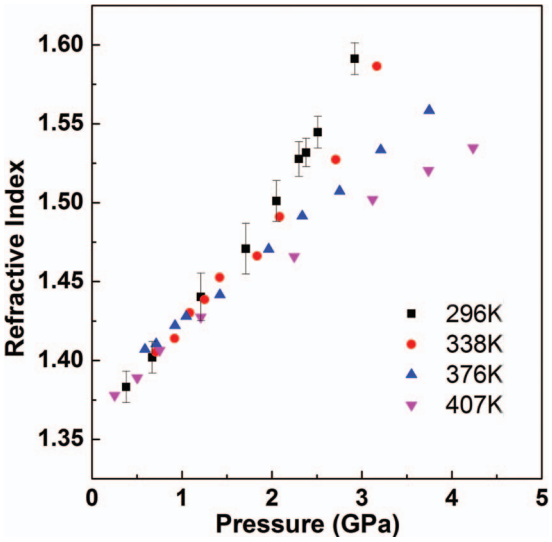

FIG. 3. The refractive index of liquid $NH_3 \cdot 2H_2O$ as a function of pressure along four measured isotherms.

Water is known to have a sound velocity largely dependent on Q (wave vector, i.e., on scattering angle 2θ, since Q $= 4\pi \sin\theta/\lambda$) as documented by several Brillouin light scattering studies.[26–28] This dependence is due to the presence of structural relaxation process and, specifically, to the related viscoelastic behavior in the supercooled phase at ambient pressure. As increasing pressure may cause similar effect as decreasing temperature, one could expect that such Q-dependent velocity behavior may be enhanced dramatically with pressure, especially at low temperature. Therefore, the pressure dependence of refractive index for 407 K shows a similar behavior as that of pure water or pure ammonia, while for lower temperature 296 K isotherm, the obvious increases of slope dn/dP with pressure above 1.5 GPa suggest a possible structural relaxation process or viscoelastic behavior in $NH_3 \cdot 2H_2O$, i.e., a change in the structure of the liquid.

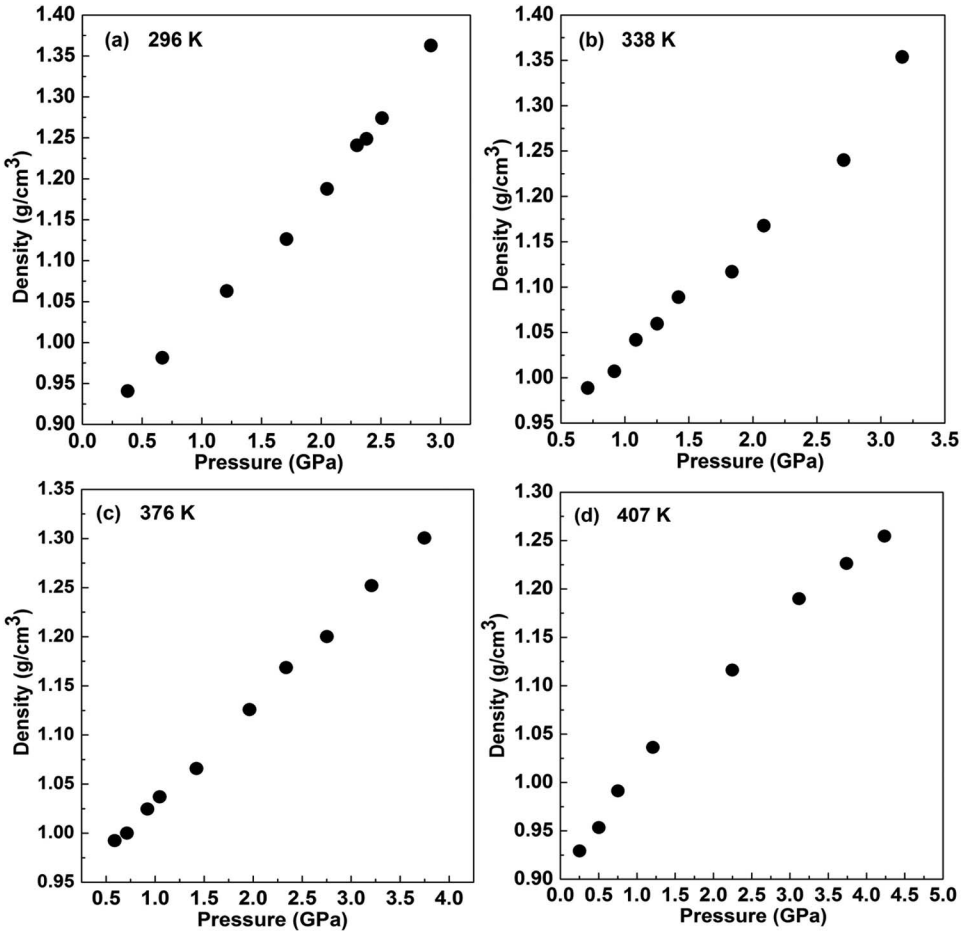

FIG. 4. Pressure evolution of the density in liquid $NH_3 \cdot 2H_2O$ at (a) 296 K, (b) 338 K, (c) 376 K, and (d) 407 K.

C. Density and bulk modulus

According to the Clausius-Mossotti (or Lorentz-Lorenz) equation,

$$(n^2 - 1)/(n^2 + 2) = (4\pi/3)(\rho/M)\alpha, \tag{3}$$

where n is refractive index, ρ is density, M is molecular weight, and α is the electronic polarizability. The refractive index is directly related to the density of materials. With initial values at a reference condition, it can be expressed as follows:

$$(\rho/\rho_0)(\alpha/\alpha_0) = \left[(n^2 - 1)\left(n_0^2 + 2\right)\right]/\left[(n^2 + 2)\left(n_0^1 - 1\right)\right], \tag{4}$$

where the subscript 0 represents a reference condition. In this work, we adopt room temperature (296 K) and ambient pressure as reference condition. With ρ_0 (296 K) = 885.2(7) kg/m^3 and by least squares fitting for the refractive index evolution with pressure, we obtained n_0 (296 K) = 1.358(2).[15,29] Therefore, the value of $\rho^*(\alpha/\alpha_0)$ as a function of pressure may be calculated on each isotherm. The variation of electronic polarizability α with pressure has been the debatable subject for a number of researchers, however, it is not yet known definitively whether the electronic polarizability in the liquid phase increases or decreases with pressure.[30] In this study on isotropic liquid phase of $NH_3 \cdot 2H_2O$, it is assumed that the electronic polarizability does not vary with pressure and temperature.[31,32] Consequently, the value of α/α_0 is eliminated from Eq. (4), so that we may obtain the density of liquid $NH_3 \cdot 2H_2O$ as a function of pressure, as shown in Figure 4. As density has relationship with volume ($\rho = M$/V, ρ is density, M is molecular weight, V is molecular volume), the ambient pressure volume of liquid $NH_3 \cdot 2H_2O$ at four different temperatures is obtained and listed in Table II.

The elastic property plays an important role in better understanding and interpreting intrinsic properties of materials. It can also provide valuable information for the intermolecular forces. In the isotropic liquid, the elastic property is described by only one parameter C_{11}, which is equivalent to the adiabatic bulk modulus B, denoted as

$$B = C_{11} = \rho V^2, \tag{5}$$

TABLE II. The ambient pressure volume (V_0), adiabatic bulk modulus (B_0) values of liquid ammonia *di*hydrate ($NH_3 \cdot 2H_2O$), and their pressure derivatives at four different temperatures; errors are shown by values in bracket.

Temperature (K)	V_0 (Å^3)	B_0 (GPa)	dB/dP
296	97.47(34)	1.50(52)	6.83(29)
338	95.17(65)	2.89(31)	6.15(17)
376	92.22(40)	4.95(11)	5.13(05)
407	94.16(98)	5.14(40)	4.41(36)

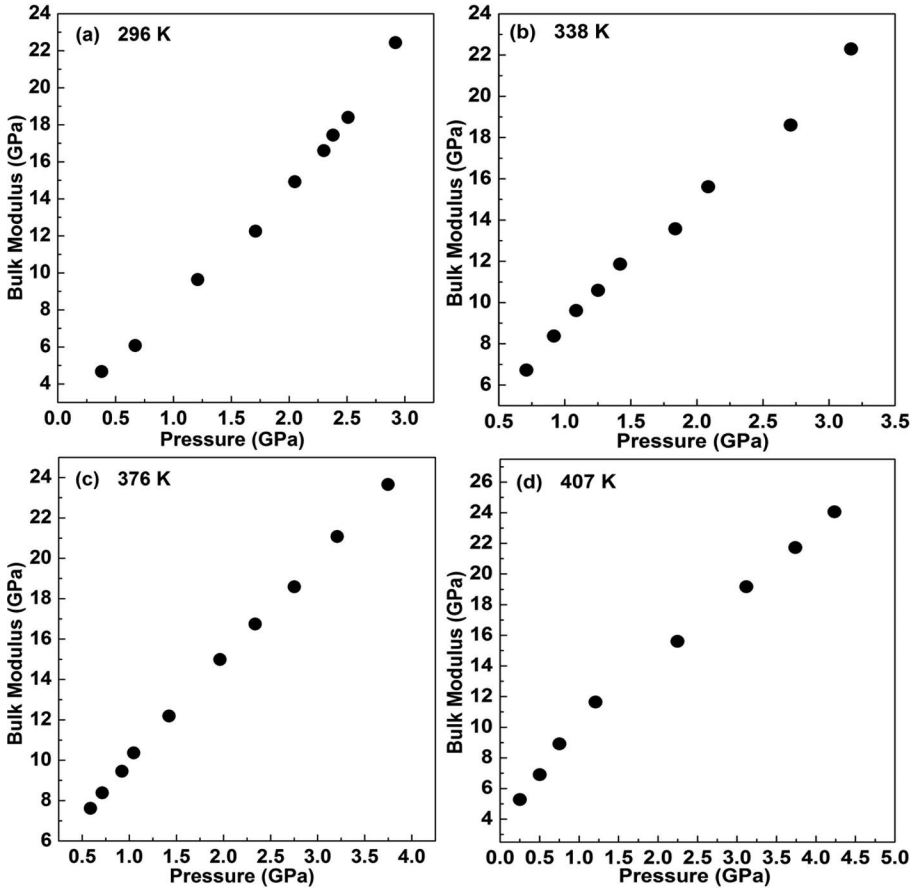

FIG. 5. The adiabatic bulk modulus of liquid $NH_3 \cdot 2H_2O$ as a function of pressure along the four measured isotherms (a) 296 K, (b) 338 K, (c) 376 K, and (d) 407 K.

where ρ represents the density and V is the acoustic velocity. The pressure dependence of adiabatic bulk modulus in liquid $NH_3 \cdot 2H_2O$ is exhibited in Figure 5. It can be seen that the adiabatic bulk modulus increases not linearly with increasing pressure on each isotherms. After linear fitting data in the whole pressure range, the adiabatic bulk modulus of liquid $NH_3 \cdot 2H_2O$ at ambient pressure and pressure derivatives along four isotherms is obtained and presented in Table II. The incompressibility of liquid $NH_3 \cdot 2H_2O$ increases with the increasing temperature. In this work, the bulk modulus B_0 for liquid $NH_3 \cdot 2H_2O$ at 296 K is 1.50 GPa, which is smaller than that had been reported at 298 K (B_0 = 2.4 GPa).[15] However, considering the possible structure change of liquid sample above 1.5 GPa as described in Sec. II, the linear fitting of bulk modulus data below 1.5 GPa result in B_0 = 2.23 (52) GPa at 296 K, which is much consistent with Croft's result in Ref. 15.

As listed in Table II, the slope of dB/dP of liquid $NH_3 \cdot 2H_2O$ in the full pressure range decreases with increasing temperature from 6.83 at 296 K to 4.41 at 407 K, which indicates that the elastic constants of $NH_3 \cdot 2H_2O$ change more with pressure at room temperature than at high temperature. This behavior is analogous to that pure liquid ammonia and high density water, whose slope of dB/dP decreases from 6.67 to 5.94 and 6.92 to 6.13 during the same temperature range.[16,19] At 296 K, the dB/dP slope sequence is H_2O>$NH_3 \cdot 2H_2O$>NH_3, and H_2O>NH_3>$NH_3 \cdot 2H_2O$ at 407 K. The dB/dP at constant temperature affects the acoustic velocity as a function of pressure, and they are in inverse relation. Through comparing with pure ammonia and pure water at a similar pressure, water possesses the maximum adiabatic bulk modulus and dB/dP slope. The larger values of water bulk modulus suggest that it is harder to compress. The dB/dP slope difference of $NH_3 \cdot 2H_2O$ and water becomes larger with increasing temperature. In view of the comparisons of the pressure dependence of elastic anisotropy, the compression behaviors of high-pressure and high-temperature liquid, maybe, have a relationship with hydrogen bond.[33] In the room-temperature and ambient-pressure liquid $NH_3 \cdot 2H_2O$, ammonia and water molecules interact with each other through multiple type of hydrogen bonds, except those in pure water or ammonia, N–H$\cdots$O and O–H$\cdots$N hydrogen bonds are included. So, the acoustic velocity of $NH_3 \cdot 2H_2O$ at 296 K as a function of pressure is a little higher than water and much lower than ammonia. When temperature increases, the ratio of multiple hydrogen bonds can be modified, the hydrogen bonds between ammonia and water are intensive, and the pressure dependence of $NH_3 \cdot 2H_2O$ acoustic velocity becomes the highest at 407 K. On the other hand, B_0 of liquid $NH_3 \cdot 2H_2O$ is found to increase with temperature as shown in Table II, however, for most materials, the bulk modulus decreases when temperature increases at ambient pressure.[34,35] Considering the B_0 for pure ammonia is smaller than pure wa-

ter also indicates possible change of hydrogen bonds' type in the system. To fully understand the influences of the H bond on the molecular liquid interaction, further experimental and theoretical investigations and comparisons are necessary.

IV. CONCLUSION

In situ high-pressure and high-temperature Brillouin scattering studies were performed on liquid $NH_3 \cdot 2H_2O$ in both back-scattering and symmetric platelet-scattering geometries. The changes of acoustic velocity and refractive index as a function of pressure have been obtained along four isotherms at 296, 338, 376, and 407 K, up to the freezing points. The acoustic velocity increases smoothly with increasing pressure at each temperature, but decreases slightly with the increased temperature at a given pressure. The refractive index on each of the four isotherms exhibits a change in slope around 1.5 GPa, indicating a possible change in the structure of the liquid. Using the Clausius–Mossotti equation, the density of liquid $NH_3 \cdot 2H_2O$ has been determined. Comparing with pure ammonia and pure water, the elastic properties of liquid $NH_3 \cdot 2H_2O$ are analyzed, which indicates different hydrogen bonds effect in each system. These results will have a significant impact on understanding of the pressure- and temperature-induced molecular structure changes of the ammonia-water binary system, and will further help in exploration of the physical state of the outer planets and their large icy satellites.

ACKNOWLEDGMENTS

This work was supported in part by the National Natural Science Foundation of China (NNSFC) (Grant Nos. 91014004, 11004074, 10574054, and 10976011), the specialized Research Fund for the Doctoral Program of Higher Education (SRFDP) (Grant No. 20100061120093), and the National Basic Research Program of China (Grant No. 2011CB808200).

[1] C. Cavazzoni, G. L. Chiarotti, S. Scandolo, E. Tosatti, M. Bernasconi, and M. Parrinello, Science **44**, 283 (1999).
[2] W. B. Hubbard, Science **214**, 145 (1981).
[3] G. I. G. Griffiths, A. D. Fortes, C. J. Pickard, and R. J. Needs, J. Chem. Phys. **136**, 174512 (2012).
[4] A. D. Fortes, E. Suard, M.-H. Lemée-Cailleau, C. J. Pickard, and R. J. Needs, J. Chem. Phys. **131**, 154503 (2009).
[5] A. D. Fortes, E. Suard, M.-H. Lemée-Cailleau, C. J. Pickard, and R. J. Needs, J. Am. Chem. Soc. **131**, 13508 (2009).
[6] A. D. Fortes, I. G. Wood, M. Alfredsson, L. Vočadlo, K. S. Knight, W. G. Marshall, M. G. Tucker, and F. Fernandez-Alonso, High Press. Res. **27**, 201 (2007).
[7] A. D. Fortes, I. G. Wood, J. P. Brodholt, M. Alfredsson, L. Vočadlo, G. S. McGrady, and K. S. Knight, J. Chem. Phys. **119**, 10806 (2003).
[8] A. D. Fortes, J. P. Brodholt, I. G. Wood, L. Vočadlo, and H. D. B. Jenkins, J. Chem. Phys. **115**, 7006 (2001).
[9] J. S. Loveday and R. J. Nelmes, Phys. Rev. Lett. **83**, 4329 (1999).
[10] J. E. Bertie and M. R. Shehata, J. Chem. Phys. **81**, 27 (1984).
[11] J. S. Loveday and R. J. Nelmes, Phys. Chem. Chem. Phys. **10**, 937 (2008).
[12] C. W. Wilson, C. L. Bull, G. Stinton, and J. S. Loveday, J. Chem. Phys. **136**, 094506 (2012).
[13] A. D. Fortes, I. G. Wood, L. Vocadlo, K. S. Knight, W. G. Marshall, M. G. Tucker, and F. Fernandez-Alonso, J. Appl. Crystallogr. **42**, 846 (2009).
[14] C. L. Ma, F. F Li, Q. Zhou, F. X. Huang, J. S. Wang, M. Z. Zhang, Z. W. Wang, and Q. L. Cui, RSC Adv. **2**, 4920 (2012).
[15] S. K. Croft, J. I. Lunine, and J. S. Kargel, Icarus **73**, 279 (1988).
[16] F. F. Li, Q. L. Cui, Z. He, T. Cui, J. Zhang, Q. Zhou, and G. T. Zou, J. Chem. Phys. **123**, 174511 (2005).
[17] H. K. Mao, J. Xu, and P. M. Bell, J. Geophys. Res. **91**, 4673, doi:10.1029/JB091iB05p04673 (1986).
[18] D. D. Ragan, R. Gustavsen, and D. Schiferl, J. Appl. Phys. **72**, 5539 (1992).
[19] F. F. Li, M. Li, Q. L. Cui, T. Cui, Z. He, Q. Zhou, and G. T. Zou, J. Chem. Phys. **131**, 134502 (2009).
[20] M. Li, F. F. Li, W. Gao, C. L. Ma, L. Y. Huang, Q. Zhou, and Q. L. Cui, J. Chem. Phys. **133**, 044503 (2010).
[21] S. Boone and M. F. Nicol, Proc. Lunar Planet Sci. **21**, 603 (1991).
[22] J. R. Sandercock, Opt. Commun. **2**, 73 (1970).
[23] A. Polian, J. Raman Spectrosc. **34**, 633 (2003).
[24] C. H. Whitfield, E. M. Brody, and W. A. Bassett, Rev. Sci. Instrum. **47**, 942 (1976).
[25] E. S. Zouboulis, M. Grimsditch, A. K. Ramdas, and S. Rodriguez, Phys. Rev. B **57**, 2889 (1998).
[26] G. Maisano, P. Migliardo, F. A liotta, C. Vasi, F. Wanderlingh, and G. D'Arrigo, Phys. Rev. Lett. **52**, 1025 (1984).
[27] G. Maisano, D. Majolino, F. Mallamace, P. Migliardo, F. Aliotta, C. Vasi, and F. Wanderlingh, Mol. Phys. **57**, 1083 (1986).
[28] S. Magazú, G. Maisano, D. Majolino, F. Mallamace, P. Migliardo, F. Aliotta, and C. Vasi, J. Phys. Chem. **93**, 942 (1989).
[29] A. D. Fortes, I. G. Wood, J. P. Brodholt, and L. Vočadlo, Icarus **162**, 59 (2003).
[30] K. Vedam and G. A. Samara, "Refractive index of liquids at high pressures," Crit. Rev. Solid State Mater. Sci. **11**(1), 1–45 (1983).
[31] J. Xu and M. H. Manghnani, Phys. Rev. B **45**, 640 (1992).
[32] J. Xu, M. H. Manghnani, and P. Richet, Phys. Rev. B **46**, 9213 (1992).
[33] T. Kume, M. Daimon, S. Sasaki, and H. Shimizu, Phys. Rev. B **57**, 13347 (1998).
[34] E. K. Goharshadi and A. Boushehri, Aust. J. Chem. **49**, 521 (1996).
[35] J. Garai and A. Laugier, J. Appl. Phys. **101**, 023514 (2007).